

Poloxamer-Alginate In-Situ Gel Containing Glatiramer Acetate Intended for Multiple Sclerosis Treatment

Anahita Shobeirean¹, Hossein Attar^{1*}, Reyhaneh Varshochian^{2*}, Mohammad Amin Rezvanfar³

¹Department of Chemical Engineering, Science and Research Branch, Islamic Azad University, Tehran, Iran

²Department of Pharmaceutics and Pharmaceutical Nanotechnology, School of Pharmacy, Shahid Beheshti University of Medical Sciences, Tehran, Iran;

³Department of Toxicology and Pharmacology, Faculty of Pharmacy, Pharmaceutical Sciences Research Center, Tehran University of Medical Sciences, Tehran, Iran.

*Corresponding author

Abstract

As an auto-immune disease multiple sclerosis (MS) has captured serious concerns about the treatment of its relapses so far. A therapeutic formulation was used in this research, which relied on glatiramer acetate (GA) as a common medicine in dealing with relapsing-MS. In this regard, a thermosensitive in situ gel composed of poloxamer 407 (P407) and sodium alginate (SA) was designed. The response surface approach was used in order to determine the optimum formulation to accomplish the desired gelling time. There were twenty distinct test runs carried out under a variety of situations, which ultimately resulted in the optimum formulation composed of 160 mg of P407, 3 mg of SA, and 60 mg of GA.

The optimization process yielded a gelling time of 20 seconds. The P407/SA gel formulation was also evaluated in terms of chemical structure and morphology using FT-IR and SEM. In addition, the rheological properties of the drug-containing gel and blank formulation were studied. Accordingly, the storage modulus and loss modulus were evaluated at both 25 and 37°C to assess their functional properties. The findings show that this in situ gel formulation may extend the beneficial effects of GA medication, making it a viable candidate for treating MS.

Keywords: Multiple sclerosis, P407, Sodium alginate, Glatiramer acetate, Drug delivery, In situ gel

1. Introduction

Over a century ago, individuals such as Charcot, Carswell, Cruveilhier, and others characterized the clinical and pathological features of multiple sclerosis (MS) [1]. MS is most commonly diagnosed during the third and fifth decades of life, with females two to three times more likely than males to be affected[2]. It is an inflammatory and autoimmune disease that progresses over time. Immune system attacks cause demyelization and the destruction of myelinated axons in the central nervous system (CNS), which impairs and slows down nerve signals [3], [4]. Various ideas suggest that the development of MS may be influenced by genetics and immunological illnesses, including viruses, metabolic abnormalities, or environmental factors[5]. The symptoms of MS are contingent upon the specific nerves affected within the CNS and may ultimately result in sensory loss, including muscle weakness, diminished reflexes, muscle spasms, impaired mobility, lack of coordination, imbalance, speech difficulties, visual disturbances, fatigue, acute or chronic pain, and complications with bladder and bowel function[6]. In the recent decade, new medicines have greatly improved the course of MS. At present, 13 unique pharmaceuticals containing 10 various active ingredients are authorized in the European Union (EU) and the United States (US) for the management of MS[7]. These medications may be classified into first-, second-, and third-line treatments[8]. GA; commercial name Copaxone, is a primary immunomodulatory medication and a

commonly used disease-modifying medicine for decreasing relapses in individuals who have relapsing-remitting multiple sclerosis (RRMS) [7].

GA is a recognized first-line disease-modifying treatment (DMT) utilized globally for patients with RRMS[9]. GA is a normalized combining of polypeptides randomly polymerized from four L-amino acids: L-glutamic acid, L-lysine, L-alanine, and L-tyrosine, in a specified molar residue ratio of 0.14:0.34:0.43:0.09[10]. The molecular mass of the component polypeptides of GA varies from 4.7 to 11 kDa [10]. The mechanism of action of GA remains incompletely understood; nonetheless, it seems to be associated with its immunomodulatory effects and neuroprotective characteristics[11]. The normal daily dosage of GA is 20mg, administered via subcutaneous injection[12]. Following injection, GA swiftly degrades into amino acids and shorter peptides[12]. The predominant adverse effects were minor responses at the injection site, including erythema, irritation, and induration[12]. The most notable adverse event is the acute and temporary immediate post-injection reaction characterized by flushing, chest tightness, palpitations, and dyspnea. Additional documented adverse effects include temporary chest discomfort and lymphadenopathy[13].

Pharmaceutical companies are concentrating on developing new drug delivery systems for existing medications with enhanced efficacy, bioavailability, and lower dosing frequency to reduce adverse effects due to the expensive expense of acquiring new chemical entities[14]. Improvements in the drug's pharmacokinetics and tissue distribution are the primary goals of any drug delivery method[15]. The need for more patient-compliant dose forms is continuously growing, which has raised demand for their technology. The advancement of in situ gelling technologies has garnered considerable interest in recent years. In situ is a Latin term signifying 'in its original location' or 'in position' [14]. The in-situ gel drug delivery system facilitates continuous and regulated drug release, enhancing patient compliance and comfort by its unique property of transitioning from a sol to a gel state [16]. An in-situ gelling system is a formulation that exists as a solution prior to entering the body, but transforms into a gel under specific physiological conditions[17]. The sol-gel transition is influenced by several factors, including temperature, pH differences, solvent exchange, UV radiation, and the existence of certain molecules or ions[18]. By prolonging a drug's release, in situ gel adheres to and absorbs the drug in gel form, so increasing the drug's half-life in the mucosa and producing a consistent plasma drug profile in the body[19], [20]. There are a number of issues with modern scaffolds and regenerative medicine techniques that may be resolved by in situ gelling equipment. They primarily reduce the invasiveness of open surgical techniques and can adapt to intricate three-dimensional geometries, which is essential in implant medication delivery systems, trauma repair, and regeneration following tumor excision[21]. This facilitates the localized distribution of cells and growth factors, potentially resulting in expedited and comprehensive regeneration [22].

Thermoresponsive gelling systems are comprised up of polymeric liquids that change from sol to gel when the temperature changes. The minimum sol–gel transition temperature ($T_{\text{sol-gel}}$) of the polymer on its temperature concentration phase diagram is determined by the interactions between water molecules and various hydrophilic/hydrophobic segments in the polymeric chain, which is known as the lower critical solution temperature (LCST)[23], [24]. Numerous natural and synthetic polymers demonstrate thermoresponsive gelling behavior at temperatures that are comparable to body temperature. Therefore, they can be employed as injectable solutions or ocular drops to achieve extended drug delivery[25].

Poloxamers are synthetic compounds that are utilized in a variety of pharmaceutical and medical purposes due to their finely flexible $T_{\text{sol-gel}}$ [26]. Poloxamer is a three-block non-ionic manufactured copolymer made up of two hydrophilic poly (ethylene oxide) blocks with a hydrophobic poly (propylene oxide) (PEO–PPO–PEO)[27], [28], [29], [30]. Poloxamer-based delivery systems exhibit thermo-responsive sol-to-gel transition behavior at concentrations beyond a critical threshold, and they may transport hydrophilic and hydrophobic medications[31]. These properties make them attractive candidates for many drug delivery applications. For ease of administration, they can be engineered to stay liquid at room temperature; nevertheless, they solidify at higher temperatures, like body temperature, producing a semisolid gel depot[31].

Within this copolymer family, poloxamer 407 (P407) exists as a non-ionic surfactant exhibiting reversible gelation characteristics under specific polymer concentrations and temperatures[32]. P407 is one of the most often utilized

poloxamers in drug delivery due to its excellent water solubility, clarity of aqueous solutions, viscosity that depends on concentration, and shear-thinning properties of its aqueous solutions[25].

Nonetheless, the elevated aqueous solubility, rapid dissolution, and unstable rheological characteristics of P407 have prompted the development of hybrid systems that include other polymers, such as sodium alginate, employed for controlled delivery systems[33]. Sodium alginate (SA) is the predominant form of alginate utilized in the pharmaceutical sector and may serve to prolong medication release[34], [35]. SA is a natural anionic linear polymer derived from brown seaweed, capable of forming a stable gel[36], [37]. SA consists of two monomeric types: beta-D-mannuronic acid (M) and alpha-L-guluronic acid (G), which enhance the mechanical and mucoadhesive characteristics of thermosensitive (poloxamer) gels[38], [39]. Alginate has carboxyl groups that become charged at pH levels exceeding 3-4, enabling alginate soluble in neutral and alkaline circumstances, hence facilitating its extensive application[40]. Therefore, the solubility and pH responsiveness of alginate render it an excellent biomaterial for drug delivery systems[41]. Numerous studies indicate that the bioavailability of medications encapsulated in alginate hydrogels is higher than that of the free drug administered directly at the lesion site, hence enhancing healing efficacy[40].

In this work, we use a thermosensitive in situ forming gel based on P407 that has been altered by SA as a long-lasting release carrier for the delivery of GA for the first time. The optimization and statistical analysis of the P407 optimum amounts were conducted via response surface methodology (RSM) to minimize costs and the number of experiments, as it is a powerful statistical approach for analyzing the interactions of various parameters at different levels.

2. Materials and methods

2.1. Materials

SA and P407 were purchased from Sigma Aldrich. GA was gifted by Tofigh Daru research and engineering Co. For pH adjustments, diluted solutions of NaOH or HCl were used. All used solvents and materials were analytical grade.

2.2. Methods

Fourier transform infrared spectroscopy (FT-IR) (Alpha Bruker, Vertex 70, Germany) was employed for chemical identification. Field emission scanning electron microscopy (FE-SEM) (ZEISS Model-EVO18 SEM, Germany) was used to detect the morphology and the structure of the gel formulations. The oscillatory shear measurements of the gels were performed using a rotational rheometer with a plate-plate geometry (MCR 301, Anton Paar, Austria). The release of GA from the prepared formulations was determined using direct method and the samples were analyzed by high-performance liquid chromatography (HPLC) (Shimadzu UFLC, United Kingdom).

2.2.1. Preparation of formulation

The in-situ gel formulations were prepared employing the cold technique, according to our previous study[42]. First, the optimal formulation was determined without the presence of the GA by utilizing the design of experiments and the response surface method. Moreover, it was validated by doing the process three times, and in the end, the gel formulation that included the GA medicine was formed based on the ideal formulation that was recommended from the experimental design. Accordingly, defined amount of P407, SA, and GA were individually transferred into a microtube, then dissolved in 1000 microliters of distilled water, and allowed to stand for 24 - 36 hours in the refrigerator to achieved a clear solution. The microtube inversion technique was used to ascertain the gelation period and the transition from the solution phase to the gel phase. The microtubes that contained the prepared formulation were put in a water bath at a temperature of 37 °C. The fluidity of the solution was regulated by inverting the microtubes every five seconds. The time at which the solution stops flowing and become gel is referred to as the gelation time.

2.2.2. Experimental design

In this study, the experimental design was acquired based on a central composite design (CCD). Statistical analyses were conducted by the Design Expert software version 13.0.5 (Stat-Ease, USA). Several variables

including SA amounts (1.0–10.0 mg) and P407 concentration percentages (14–24 %) have been employed for modeling and optimization. The output data were fitted with various models and analysis of variance (ANOVA) was used to obtain the most appropriate one.

2.2.3. Rheology analysis

Oscillatory shear measurements were conducted using a TA Instrument Hybrid Rheometer DISCOVERY HR-3, using a plate-plate geometry (Flat Plate 40mm diameter) and a Peltier system for temperature regulation. The storage (G') and loss moduli (G'') were assessed over the angular frequency (ω) spectrum of 0.01 to 100. In these studies, the Storage modulus (G') and loss modulus (G'') were observed as a function of frequency inside the linear viscoelastic domain at different temperatures[43].

2.2.4. In vitro release profile of GA formulation

The release samples were evaluated using HPLC employing a PWXL TSKgel G3000PWXL 7.8 ID \times 30.0 L 500-80,000 column (column temperature: 30 °C, flow rate: 0.5 mL/min, UV Detector: 235 nm), with the mobile phase consisting of a Buffer/Acetonitrile combination (95/5).

After placing an exact amount of the drug-loaded formulation, which contained 20 mg of GA, into the bottom of a tube and allowing it to reach a temperature of 37 °C in a water bath, a gel network was generated. After that, 10 ml of phosphate buffered saline (PBS) with a temperature of 37 °C and a pH of 7.4 was slowly added on the surface of the gel layer. Finally, the tubes were set in an incubator that was shaking. Because of preserving the sink condition and maintaining a consistent volume, the release samples were collected at specified time intervals and replaced with fresh PBS at a temperature of 37° Celsius.

3. Results and discussion

3.1. FT-IR spectroscopy characterization

Fig.1 demonstrates FT-IR spectra (4000–400 cm^{-1}) of the GA, SA, P407 and the composite (GA/SA/P407). The FT-IR spectrum of the provided composite clearly displays the peaks at 1089 cm^{-1} , 1393 cm^{-1} , 1540 cm^{-1} , 1647 cm^{-1} , 2943 cm^{-1} , and 3360 cm^{-1} . The peaks at 1089 cm^{-1} and 1393 cm^{-1} correspond to C-O-C stretching vibration and carboxylate, respectively[44]. Additionally, the presence of the amide functional group, shown by the peak at 1540 cm^{-1} , confirms the existence of the GA medicine in the synthesized composite structure[45]. Furthermore, the carbonyl functional group resulted in a peak at 1647 cm^{-1} , while bands at 2943 cm^{-1} and 3360 cm^{-1} correspond to CH_2 stretching vibration and O-H absorption, respectively[46]. Moreover, the peaks related to the SA and P407 with a slight shift are clearly observable in the composite spectrum. Consequently, it can be concluded that the structures of polymers and the drug were all preserved in final gel product.

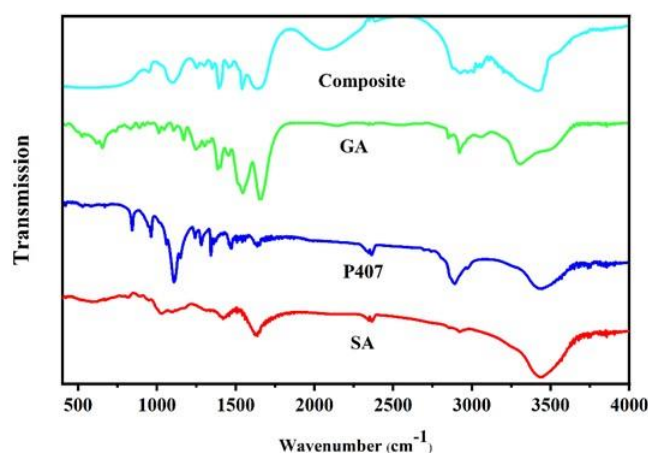


Fig. 1. FT-IR spectra of P407, SA, GA and the composite (the optimum gel containing GA)

3.3. Morphology of the gel formulation

Fig.2a and **2b** illustrate the morphology of samples obtained from the gel without GA and the gel containing GA, respectively. **Fig.2a** clearly exhibits the sheet-like and flat structure of the gel, indicating the homogenous composition of the components (P407 and SA) in the absence of GA. **Fig.2b** depicts the flaky structure of the synthesized gel. The alteration in structure and morphology on the gel's surface signifies the presence of the GA drug and the effective integration of the drug with the gel matrix.

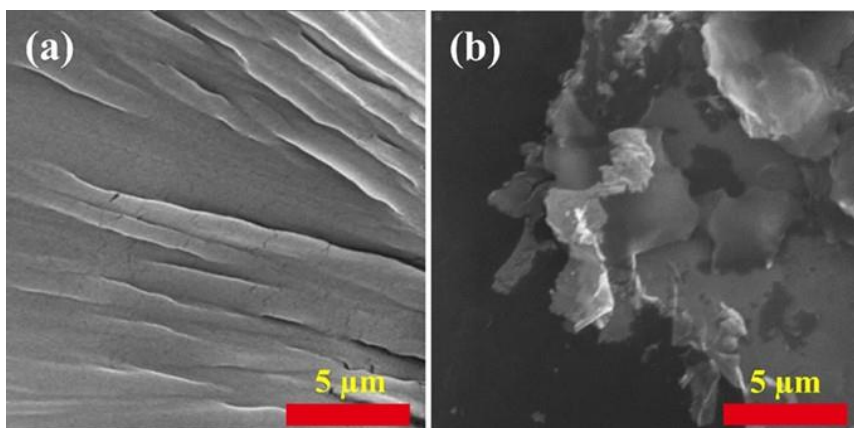


Fig. 2.a FE-SEM images of unloaded and **(b)** GA-loaded gel with different magnifications

3.2. RSM modeling and statistical analysis

The data were examined to identify the optimal model. RSM is a suitable approach for examining the relationship between the parameters referenced[47]. The analysis of variance (ANOVA) results (**Table 1**) indicate that the quadratic model is suitable for characterizing the relationship between the variables in the in-situ gelling drug delivery process. The equation of the derived model expressed in coded variables is (**Eq. 1**):

$$\text{Gelling Time (s)} = + 14.64 - 9.04 A - 8.08 B + 1.5 AB + 1.57 B^2 \quad \text{Eq. 1}$$

Where A and B are SA and P407, respectively.

The effectiveness of the suggested model is shown by the statistically significant coefficient of determination ($R^2 = 0.9623$) and the insignificant P-value (<0.0001). The term "adequate precision" (AP) refers to a metric that is used to evaluate the signal-to-noise ratio[48]. It is generally accepted that a ratio that is larger than four is ideal. In the study that was done, the quadratic model was able to reach a signal-to-noise ratio of 33.164, which was quite adequate.

Table 1. ANOVA of the reduced cubic model

Source	Sum of Squares	df	Mean Square	F-value	p-value	Significancy
Model	1631.02	4	407.75	95.59	< 0.0001	significant
A-SA	893.29	1	893.29	209.42	< 0.0001	
B-P407	713.87	1	713.87	167.36	< 0.0001	
AB	9.00	1	9.00	2.11	0.1669	
B²	14.86	1	14.86	3.48	0.0817	
Residual	63.98	15	4.27			
Lack of Fit	52.57	4	13.14	12.66	0.0004	significant
Pure Error	11.42	11	1.04			
Cor Total	1695.00	19				

For the purpose of determining whether or not the mathematical models are adequate, the correlation between the actual values and the predicted values was investigated. A fair agreement may be said to exist between the Predicted R^2 (0.8966) and the Adjusted R^2 (0.9522) since the difference between the two is less than 0.2. The

association between actual and expected responses demonstrated the appropriateness of the generated mathematical model for representing anticipated results.

Fig.3a and **3b** illustrate the three-dimensional diagram and contour plot of the mutual effects resulting from differences in the amounts of SA and P407 during gelation. The range of changes in P407 amounts was assessed between 14% and 24%, whereas SA amounts ranged from 1 to 10 mg. The gelation time is reduced by increasing the quantity of P407 to the point where it drops to 1 or 2 seconds in levels of 24% by weight. This short duration hinders the efficient distribution of the drug and interrupts the drug delivery system. However, increasing the amount of SA also slightly shortens the gelation duration. The optimal concentrations of SA and P407 were determined to be 3 mg and 19%, respectively, in order to obtain a gelation time of 20 s and optimal drug delivery performance. The optimization process is conducted by utilizing the desirability factor, which is a number between 0 and 1. In this case, we took into account the highest desirability factor, which is 1.

Finally, according to the experimental design outcomes the optimum formulation composed of 160 mg of P407, 3 mg of SA, and 60 mg of GA was prepared which accepted with the predicted gelling time values.

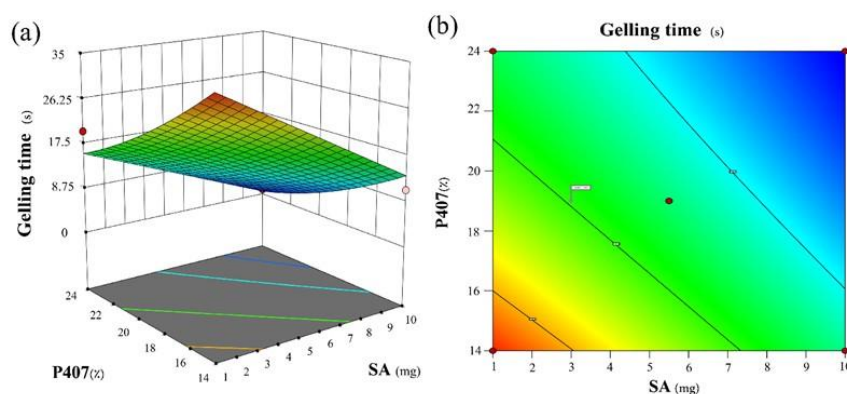


Fig.3. (a) 3d diagram and **(b)** contour plot of the Interactive effects of P407 and SA on gelling time

3.4. Rheology analysis

Various experiments are performed on rheometers based on the study's objectives. The oscillating amplitude test is conducted to identify the linear viscoelastic region (LVR) in which stress and strain exhibit a linear relationship. The oscillating frequency test evaluates the impact of angular frequency on complex modulus to determine gel strength over short and long durations. The storage modulus indicates a material's elasticity or rigidity. Elastic materials undergo immediate deformation with the application of shear stress. G' is a quantification of a material's viscosity or fluidity. Gels are solid-like materials; hence, G' should surpass G'' [49].

The point at which G' is equal to G'' is often utilized to denote the time when the material deforms and subsequently flows[50].

Detecting the change in viscoelastic characteristics as a consequence of temperature was used to evaluate the gelation process that the formulations underwent. As a function of temperature, the elastic and viscous moduli of unloaded and GA-loaded formulations can be seen in **Fig.4**. based on the frequency value of 1 Hz. The temperature at which the G' and G'' curves intersect with one another is known as the gelation temperature, abbreviated as T_{gel} . The intersection points of G' and G'' may be ascribed to the generation of hydrophobic regions inside the polymeric network during the initial phases of gelation growth[51]. **Fig.4** indicates that the T_{gel} of the unloaded formulation and the GA-loaded formulation were approximately 36 °C and 37 °C, respectively, demonstrating comparable gelation characteristics.

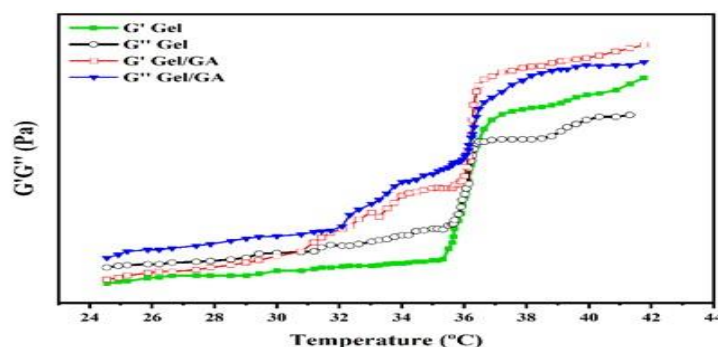
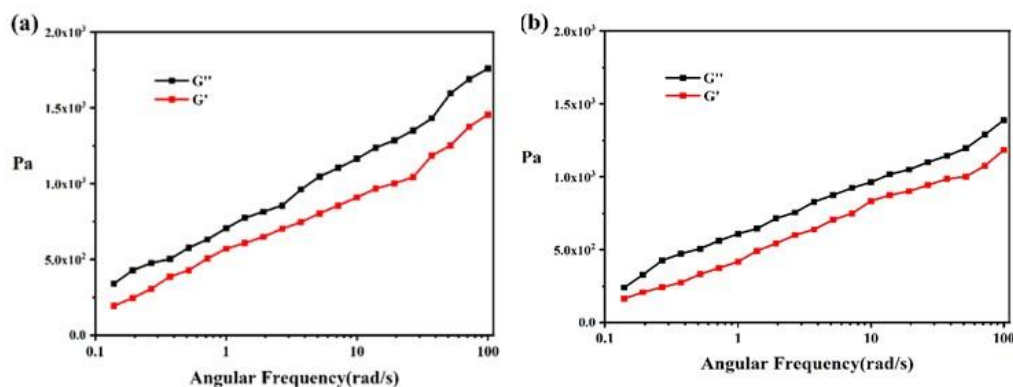


Fig.4 The G' (storage modulus) and the G'' (loss modulus) of unloaded and GA-loaded gel formulations at different temperature

As can be seen in **Fig.4**, the rheological results indicate that the patterns of G' and G'' parameters based on the temperature are similar in both loaded and unloaded gel formulations, which can be attributed to their similar gel formation behavior. At temperatures exceeding 37°C , G' surpassed G'' , indicating that the formulation demonstrated energy-saving capabilities and exhibited a lower susceptibility to deformation. On the other hand, the formulation exhibited viscous liquid-like behavior at temperatures below 37°C , where G'' was greater than G' . The synergy between the thermosensitive properties of P407 and the SA characteristics, as well as the impact of SA on the P407 gelification process, can be seen by the given graph.

Fig.5a-5d illustrate the rheological characteristics of the prepared gel as a function of angular frequency (ω) at temperatures of 25°C and 37°C , both in the presence and absence of the medication.

This test evaluates the elastic response component (G' , storage modulus) and the viscous response component (G'' , loss modulus) of formulations. G' quantifies the deformation energy retained during shear, reflecting the sample's stiffness, whereas G'' quantifies the energy released during shear, indicating the sample's liquid-like behavior. If $G'' > G'$, the formulation exhibits characteristics of a viscous liquid; conversely, if $G'' < G'$, it demonstrates properties of an elastic solid[52]. At a temperature of 25°C , both the drug-containing and drug-free gels exhibit G'' values exceeding G' values within the frequency range of 0.1 to 100, indicating the gels' viscous nature ($G' < G''$). **Fig.5a** and **5b** demonstrate that the G' and G'' values of both loaded and unloaded gel samples rose with an increase in angular frequency (ω). As seen in **Fig.5c** and **5d**, at a temperature of 37°C , the storage modulus exhibited greater values than the loss modulus throughout all frequency ranges, indicating enhanced mechanical strength at this temperature[53], [54]. Furthermore, no detrimental change was noted in the G' and G'' values, indicating that G' values consistently exceeded G'' values across the entire frequency spectrum examined. This demonstrates that the gel solutions displayed a solid-like behavior ($G' > G''$) at the physiological body temperature due to the weak association of ordered chains [55], [56]. In contrast to the results at 25°C , the G' and G'' values of the samples at 37°C were rather stable throughout all angular frequency levels. This suggests that the rheological characteristics are comparable to those of substances that have a gel like structure.



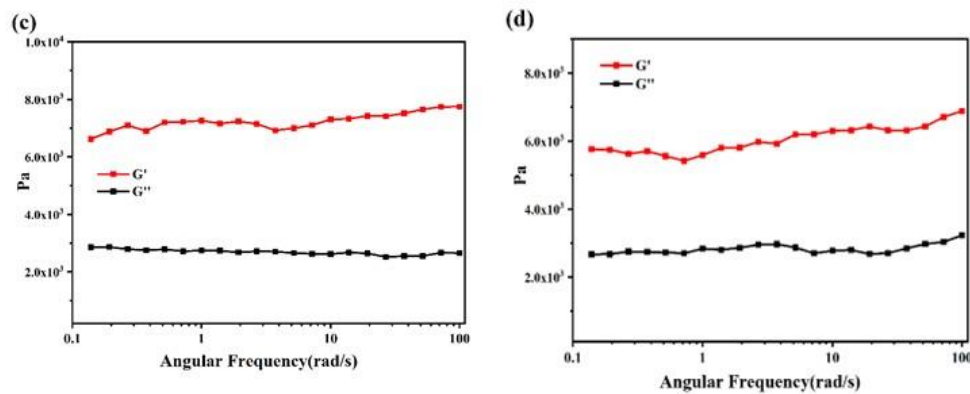


Fig.5 The G' (storage modulus) and the G'' (loss modulus) of gel formulations based on angular frequency of unloaded gel (a), loaded gel (b) at 25 °C, and unloaded gel (c), loaded gel (d) at 37 °C

Fig.6a and **6b** illustrate the gel's behavior at various shear rates in the presence of GA medicine and without it. The test was conducted at two temperatures: 25 °C (ambient temperature) and 37 °C (physiological body temperature). All samples show a steadily increasing shear stress with a corresponding enhancement in the shear rate. At a temperature of 25 °C, the shear stress of the unloaded gel increased by over 1000 units, while in the presence of GA at the same shear rates, it increased by over 3000 units. As can it be seen in **fig.6c** and **6d**, the loaded gel's shear stress, at an operating temperature of 37°C, is five times higher than the sample's shear stress without GA, which reached 4500 (D/cm²) at a shear rate of 920 (1/sec). Based on the results, the generated gel exhibits non-Newtonian behavior and possesses pseudoplastic characteristics. The shear rate and shear stress data that were obtained are in agreement with Bingham's models and indicate the pseudo-plastic behavior of the gel formulations[57].

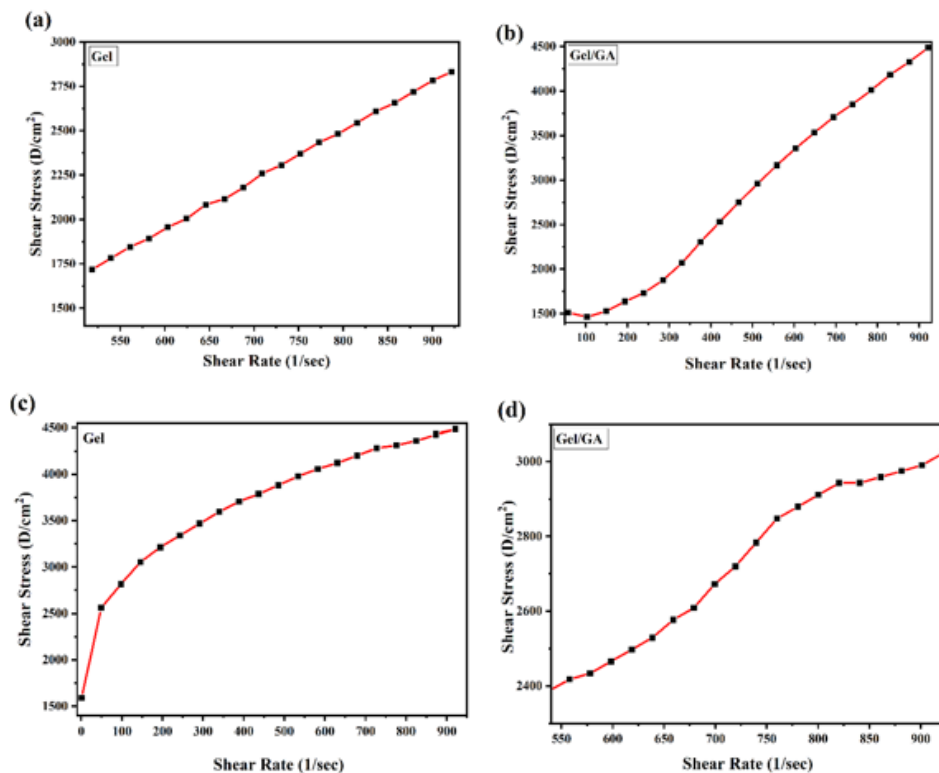


Fig.6 The shear stress based on shear rates charts of unloaded and loaded gel at 25 °C (a), (b) and at 37 °C (c), (d)

3.5. Analysis of the in vitro release profile of GA in the gel formulation

Fig.7 illustrates the in vitro drug release kinetics achieved under physiological circumstances (37°C, PBS at pH 7.4) for a duration of 240 hours. The assessment of the GA measurement in the final formulation and the study of the release pattern were conducted using HPLC. A calibration curve was created with particular amounts of GA ranging from 0.6 to 60 mg/ml, displayed across the corresponding area under the curve (AUC). The results of the study indicated that $99.2 \pm 1.22\%$ of the used GA was incorporated into the final formulation. Once the first hour had passed, the burst release of around 24% was detected. Despite the fact that the drug release during the first 24 hours was somewhat rapid, it continued to increase in a gradual pattern throughout the remaining hours of the test, with a median slope of $0.05 \text{ mg/mlhr}^{-1}$. The type of substance, network structure, polymer classification, and interactions between molecules in the drug-hydrogel matrix all influence how a drug release.

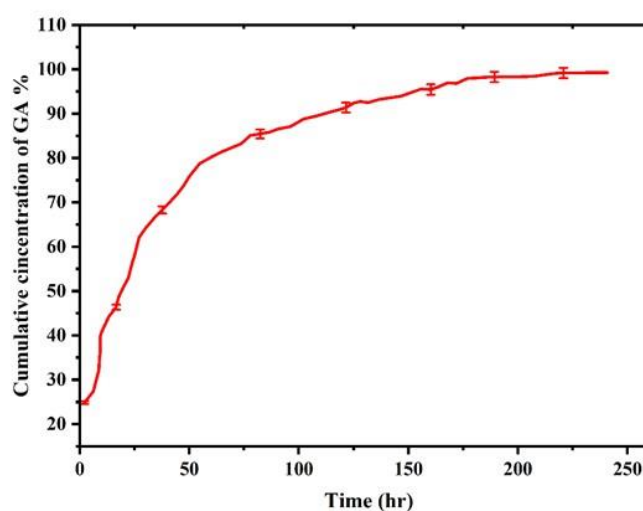


Fig.7 The profile for the in vitro cumulative percent of released GA from P407/SA gel versus time at 37 °C

Conclusion

The present study describes the effective development of a thermosensitive in-situ gel formulation containing GA, a peptidic pharmaceutical intended for treatment of MS. P407 and SA were utilized to prepare the formulation. To determine the ideal gelling time with optimum amounts of SA and P407, the CCD experimental design was used. The obtained temperature sensitive gelling procedure together with the suitable gelling time, FE-SEM images and FT-IR outcomes, confirmed the successful fabrication of the in-situ gel formulation. Rheological tests were performed on the gel formulation as the last phase. Finally, the gel formulation demonstrated a controlled release profile within time which suggests that it has the potential to be used as a novel and dependable approach to the treatment of multiple MS.

References

- [1] W. I. McDonald, F. Fazekas, and A. J. Thompson, "Chapter 1 The Diagnosis of Multiple Sclerosis," 2003, pp. 1–11. doi: 10.1016/S1877-3419(09)70030-3.
- [2] P. E. M. van Schaik, I. S. Zuhorn, and W. Baron, "Targeting Fibronectin to Overcome Remyelination Failure in Multiple Sclerosis: The Need for Brain- and Lesion-Targeted Drug Delivery," Aug. 01, 2022, *MDPI*. doi: 10.3390/ijms23158418.
- [3] A. Singh, P. Zamboni, and M. Khare, "Prospect of brain-machine interface in motor disabilities: The future support for multiple sclerosis patient to improve quality of life," *Ann Med Health Sci Res*, vol. 4, no. 3, p. 305, 2014, doi: 10.4103/2141-9248.133447.
- [4] A. Compston and A. Coles, "Multiple sclerosis," *The Lancet*, vol. 372, no. 9648, pp. 1502–1517, Oct. 2008, doi: 10.1016/S0140-6736(08)61620-7.

- [5] S. Ojha and B. Kumar, "A review on nanotechnology based innovations in diagnosis and treatment of multiple sclerosis," *Journal of Cellular Immunotherapy*, vol. 4, no. 2, pp. 56–64, Dec. 2018, doi: 10.1016/j.jocit.2017.12.001.
- [6] K. M. M. Koriem, "Multiple sclerosis: New insights and trends," *Asian Pac J Trop Biomed*, vol. 6, no. 5, pp. 429–440, May 2016, doi: 10.1016/j.apjtb.2016.03.009.
- [7] L. De Riccardis *et al.*, "Metabolic response to glatiramer acetate therapy in multiple sclerosis patients," *BBA Clin*, vol. 6, pp. 131–137, Dec. 2016, doi: 10.1016/j.bbacli.2016.10.004.
- [8] T. Berger, "Current therapeutic recommendations in multiple sclerosis," *J Neurol Sci*, vol. 287, pp. S37–S45, Dec. 2009, doi: 10.1016/S0022-510X(09)71299-7.
- [9] A. L. Boster, C. C. Ford, O. Neudorfer, and Y. Gilgun-Sherki, "Glatiramer acetate: long-term safety and efficacy in relapsing-remitting multiple sclerosis," *Expert Rev Neurother*, vol. 15, no. 6, pp. 575–586, Jun. 2015, doi: 10.1586/14737175.2015.1040768.
- [10] G. Comi *et al.*, "The heritage of glatiramer acetate and its use in multiple sclerosis," *Mult Scler Demyelinating Disord*, vol. 1, no. 1, p. 6, Dec. 2016, doi: 10.1186/s40893-016-0010-2.
- [11] G. Izquierdo, N. García-Agua Soler, M. Rus, and A. J. García-Ruiz, "Effectiveness of glatiramer acetate compared to other multiple sclerosis therapies," *Brain Behav*, vol. 5, no. 6, Jun. 2015, doi: 10.1002/brb3.337.
- [12] T. Ziemssen, O. Neuhaus, and R. Hohlfeld, "Risk-Benefit Assessment of Glatiramer Acetate in Multiple Sclerosis," *Drug Saf*, vol. 24, no. 13, pp. 979–990, 2001, doi: 10.2165/00002018-200124130-00005.
- [13] G. Marco-Martín, P. Tornero, A. Prieto, A. La Rotta, T. Herrero, and M. L. Baeza, "Immediate reactions with glatiramer acetate," *Neurol Clin Pract*, vol. 10, no. 2, pp. 170–177, Apr. 2020, doi: 10.1212/CPJ.0000000000000714.
- [14] Soniya R. Devasani, S. R. Asish Dev, and Ganesh Deshmukh, "An overview of in situ gelling systems ," *PHARMACEUTICAL AND BIOLOGICAL EVALUATIONS*, vol. 3, no. 1, pp. 60–69, Feb. 2016.
- [15] ASMITA SINGH, PRERANA VENGURLEKAR, and SUDHA RATHOD, "DESIGN, DEVELOPMENT AND CHARACTERIZATION OF LIPOSOMAL NEEM GEL," *International Journal of Pharma Sciences and Research (IJPSR)* , vol. 5, no. 4, pp. 140–148, Apr. 2014.
- [16] Mayuri R. Khule and Sachin B. Vyavahare, "A Review: in-situ Gel Drug Delivery System," *International Journal of All Research Education and Scientific Methods (IJARESM)*, vol. 9, no. 3, pp. 899–909, Mar. 2021.
- [17] B. J. Shaikh, I. D. Raut, M. M. Nitalikar, S. K. Mohite, and C. S. Magdum, "An Overview on In-Situ Gel: A Novel Drug Delivery System," *International Journal of Pharmaceutical Sciences and Nanotechnology(IJPSN)*, vol. 15, no. 5, pp. 6180–6189, Oct. 2022, doi: 10.37285/ijpsn.2022.15.5.10.
- [18] Sarada K, Firoz S, and Padmini K, "In-Situ Gelling System: A Review," *International Journal of Current Pharmaceutical Review and Research*, vol. 5, no. 4, pp. 76–90, Nov. 2014.
- [19] B. Padmasri, R. Nagaraju, and D. Prasanth, "A comprehensive review on in situ gels," Nov. 01, 2020, *Innovare Academics Sciences Pvt. Ltd.* doi: 10.22159/ijap.2020v12i6.38918.
- [20] Lovenish Bhardwaj, Pramod Kumar Sharma, and Rishabha Malviya, "A Short Review on Gastro Retentive Formulations for Stomach Specific Drug Delivery: Special Emphasis on Floating In situ Gel Systems," *African Journal of Basic & Applied Sciences* , vol. 3, no. 6, pp. 300–311, 2011.
- [21] L. Liu, Q. Gao, X. Lu, and H. Zhou, "In situ forming hydrogels based on chitosan for drug delivery and tissue regeneration," *Asian J Pharm Sci*, vol. 11, no. 6, pp. 673–683, Dec. 2016, doi: 10.1016/j.ajps.2016.07.001.

- [22] T. Russo, M. Tunesi, C. Giordano, A. Gloria, and L. Ambrosio, "Hydrogels for central nervous system therapeutic strategies," *Proc Inst Mech Eng H*, vol. 229, no. 12, pp. 905–916, Dec. 2015, doi: 10.1177/0954411915611700.
- [23] D. López, A. Saiani, and J.-M. Guenet, "Temperature-Concentration Phase Diagrams in The Study of Thermoreversible Gelation," *J Therm Anal Calorim*, vol. 51, no. 3, pp. 841–850, Mar. 1998, doi: 10.1007/BF03341461.
- [24] J. F. Mano, "Stimuli-Responsive Polymeric Systems for Biomedical Applications," *Adv Eng Mater*, vol. 10, no. 6, pp. 515–527, Jun. 2008, doi: 10.1002/adem.200700355.
- [25] K. A. Soliman, K. Ullah, A. Shah, D. S. Jones, and T. R. R. Singh, "Poloxamer-based in situ gelling thermoresponsive systems for ocular drug delivery applications," Aug. 01, 2019, *Elsevier Ltd*. doi: 10.1016/j.drudis.2019.05.036.
- [26] A. Fakhari, M. Corcoran, and A. Schwarz, "Thermogelling properties of purified poloxamer 407," *Heliyon*, vol. 3, no. 8, p. e00390, Aug. 2017, doi: 10.1016/j.heliyon.2017.e00390.
- [27] P. Alexandridis and T. Alan Hatton, "Poly(ethylene oxide)–poly(propylene oxide)–poly(ethylene oxide) block copolymer surfactants in aqueous solutions and at interfaces: thermodynamics, structure, dynamics, and modeling," *Colloids Surf A Physicochem Eng Asp*, vol. 96, no. 1–2, pp. 1–46, Mar. 1995, doi: 10.1016/0927-7757(94)03028-X.
- [28] S. M. Querobino *et al.*, "Physicochemical data of oleic acid-poloxamer organogel for intravaginal voriconazole delivery," *Data Brief*, vol. 25, p. 104180, Aug. 2019, doi: 10.1016/j.dib.2019.104180.
- [29] H. Almeida, M. H. Amaral, P. Lobão, and J. M. S. Lobo, "In situ gelling systems: a strategy to improve the bioavailability of ophthalmic pharmaceutical formulations," *Drug Discov Today*, vol. 19, no. 4, pp. 400–412, Apr. 2014, doi: 10.1016/j.drudis.2013.10.001.
- [30] A. LUDWIG, "The use of mucoadhesive polymers in ocular drug delivery," *Adv Drug Deliv Rev*, vol. 57, no. 11, pp. 1595–1639, Nov. 2005, doi: 10.1016/j.addr.2005.07.005.
- [31] H. Abdeltawab, D. Svirskis, and M. Sharma, "Formulation strategies to modulate drug release from poloxamer based in situ gelling systems," *Expert Opin Drug Deliv*, vol. 17, no. 4, pp. 495–509, Apr. 2020, doi: 10.1080/17425247.2020.1731469.
- [32] A. Fakhari, M. Corcoran, and A. Schwarz, "Thermogelling properties of purified poloxamer 407," *Heliyon*, vol. 3, no. 8, p. e00390, Aug. 2017, doi: 10.1016/j.heliyon.2017.e00390.
- [33] D. K. Khajuria and D. Roy Mahapatra, "Photonic hydrogel beads for controlled release of risedronate," B. Choi, N. Kollias, H. Zeng, H. W. Kang, B. J. F. Wong, J. F. Ilgner, G. J. Tearney, K. W. Gregory, L. Marcu, A. Mandelis, and M. D. Morris, Eds., Mar. 2014, p. 892640. doi: 10.1117/12.2042568.
- [34] M. Szekalska, A. Puciłowska, E. Szymańska, P. Ciosek, and K. Winnicka, "Alginate: Current Use and Future Perspectives in Pharmaceutical and Biomedical Applications," *Int J Polym Sci*, vol. 2016, pp. 1–17, 2016, doi: 10.1155/2016/7697031.
- [35] S. Jana, K. Kumar Sen, and A. Gandhi, "Alginate Based Nanocarriers for Drug Delivery Applications," *Curr Pharm Des*, vol. 22, no. 22, pp. 3399–3410, May 2016, doi: 10.2174/1381612822666160510125718.
- [36] X. Gao, Z. Yu, B. Liu, J. Yang, X. Yang, and Y. Yu, "A smart drug delivery system responsive to pH/enzyme stimuli based on hydrophobic modified sodium alginate," *Eur Polym J*, vol. 133, p. 109779, Jun. 2020, doi: 10.1016/j.eurpolymj.2020.109779.
- [37] S. M. Querobino *et al.*, "Sodium alginate in oil-poloxamer organogels for intravaginal drug delivery: Influence on structural parameters, drug release mechanisms, cytotoxicity and in vitro antifungal activity," *Materials Science and Engineering: C*, vol. 99, pp. 1350–1361, Jun. 2019, doi: 10.1016/j.msec.2019.02.036.

- [38] H.-R. Lin, K. C. Sung, and W.-J. Vong, "In Situ Gelling of Alginate/Pluronic Solutions for Ophthalmic Delivery of Pilocarpine," *Biomacromolecules*, vol. 5, no. 6, pp. 2358–2365, Nov. 2004, doi: 10.1021/bm0496965.
- [39] K. Kesavan, "Sodium Alginate Based Mucoadhesive System for Gatifloxacin and Its In Vitro Antibacterial Activity," *Sci Pharm*, vol. 78, no. 4, pp. 941–957, 2010, doi: 10.3797/scipharm.1004-24.
- [40] D. M. Hariyadi and N. Islam, "Current Status of Alginate in Drug Delivery," *Adv Pharmacol Pharm Sci*, vol. 2020, pp. 1–16, Aug. 2020, doi: 10.1155/2020/8886095.
- [41] M. Cardoso, R. Costa, and J. Mano, "Marine Origin Polysaccharides in Drug Delivery Systems," *Mar Drugs*, vol. 14, no. 2, p. 34, Feb. 2016, doi: 10.3390/md14020034.
- [42] A. Shobeirean, H. Attar, R. Varshochian, and M. A. Rezvanfar, "Glatiramer acetate in situ forming gel, a new approach for multiple sclerosis treatment," *DARU Journal of Pharmaceutical Sciences*, Sep. 2024, doi: 10.1007/s40199-024-00532-z.
- [43] I. A. Rodríguez *et al.*, "Rheological characterization of human fibrin and fibrin-agarose oral mucosa substitutes generated by tissue engineering," *J Tissue Eng Regen Med*, vol. 6, no. 8, pp. 636–644, Aug. 2012, doi: 10.1002/term.466.
- [44] H. Lei, M. Xie, Y. Zhao, F. Zhang, Y. Xu, and J. Xie, "Chitosan/sodium alginate modified graphene oxide-based nanocomposite as a carrier for drug delivery," *Ceram Int*, vol. 42, no. 15, pp. 17798–17805, Nov. 2016, doi: 10.1016/j.ceramint.2016.08.108.
- [45] F. Molavi, M. Barzegar-Jalali, and H. Hamishehkar, "Changing the daily injection of glatiramer acetate to a monthly long acting product through designing polyester-based polymeric microspheres," *BioImpacts*, Aug. 2022, doi: 10.34172/bi.2022.23733.
- [46] Z. M.A. Fathalla *et al.*, "Poloxamer-based thermoresponsive ketorolac tromethamine in situ gel preparations: Design, characterisation, toxicity and transcorneal permeation studies," *European Journal of Pharmaceutics and Biopharmaceutics*, vol. 114, pp. 119–134, May 2017, doi: 10.1016/j.ejpb.2017.01.008.
- [47] W.-H. Chen *et al.*, "A comprehensive review of thermoelectric generation optimization by statistical approach: Taguchi method, analysis of variance (ANOVA), and response surface methodology (RSM)," *Renewable and Sustainable Energy Reviews*, vol. 169, p. 112917, Nov. 2022, doi: 10.1016/j.rser.2022.112917.
- [48] S. Nozar, S. M. Pourmoheb Hosseini, N. Chaibakhsh, and M. Amini, "Light-assisted catalytic ozonation for efficient degradation of ciprofloxacin using NiO/MoS₂ nanocomposite," *J Photochem Photobiol A Chem*, vol. 448, p. 115343, Feb. 2024, doi: 10.1016/j.jphotochem.2023.115343.
- [49] A. Hamza, M. Shamlooh, I. A. Hussein, M. Nasser, and S. Salehi, "Polymeric formulations used for loss circulation materials and wellbore strengthening applications in oil and gas wells: A review," *J Pet Sci Eng*, vol. 180, pp. 197–214, Sep. 2019, doi: 10.1016/j.petrol.2019.05.022.
- [50] J. de Gasperi, D. Holthusen, M. F. D. Howes, N. Sattler, M. A. Longhi, and E. D. Rodríguez, "Temporal dynamics of rheological properties of metakaolin-based geopolymers: Effects of synthesis parameters," *Constr Build Mater*, vol. 289, p. 123145, Jun. 2021, doi: 10.1016/j.conbuildmat.2021.123145.
- [51] W. Ji, B. Chang, H. Yu, Y. Li, and W. Song, "Effect of Polymer and Crosslinker Concentration on Static and Dynamic Gelation Behavior of Phenolic Resin Hydrogel," *Gels*, vol. 10, no. 5, p. 325, May 2024, doi: 10.3390/gels10050325.
- [52] S. Monteiro e Silva *et al.*, "Gallic Acid-Loaded Gel Formulation Combats Skin Oxidative Stress: Development, Characterization and Ex Vivo Biological Assays," *Polymers (Basel)*, vol. 9, no. 9, p. 391, Aug. 2017, doi: 10.3390/polym9090391.

- [53] J.-L. Xu, J.-C. Zhang, Y. Liu, H.-J. Sun, and J.-H. Wang, "Rheological properties of a polysaccharide from floral mushrooms cultivated in Huangshan Mountain," *Carbohydr Polym*, vol. 139, pp. 43–49, Mar. 2016, doi: 10.1016/j.carbpol.2015.12.011.
- [54] Y. Wang, X. Li, G. Sun, D. Li, and Z. Pan, "A comparison of dynamic mechanical properties of processing-tomato peel as affected by hot lye and infrared radiation heating for peeling," *J Food Eng*, vol. 126, pp. 27–34, Apr. 2014, doi: 10.1016/j.jfoodeng.2013.10.032.
- [55] M. T. Yılmaz, G. Kutlu, E. Tulukcu, O. S. Toker, O. Sagdic, and S. Karaman, "Rheological characteristics of Salvia sclarea seed gum solutions at different hydration temperature levels: Application of three interval thixotropy test (3ITT)," *LWT - Food Science and Technology*, vol. 71, pp. 391–399, Sep. 2016, doi: 10.1016/j.lwt.2016.03.043.
- [56] S. M. A. Razavi, H. Taheri, and R. Sanchez, "Viscoelastic Characterization of Sage Seed Gum," *Int J Food Prop*, vol. 16, no. 7, pp. 1604–1619, Oct. 2013, doi: 10.1080/10942912.2011.604888.
- [57] M. Nejadmansouri, E. Shad, M. Razmjooei, R. Safdarianghomsheh, F. Delvigne, and M. Khalesi, "Production of xanthan gum using immobilized Xanthomonas campestris cells: Effects of support type," *Biochem Eng J*, vol. 157, p. 107554, Apr. 2020, doi: 10.1016/j.bej.2020.107554.